Impact of a Tethyan circumglobal passage on ocean heat transport and "equable" climates

R. M. Hotinski
Atmospheric and Oceanic Sciences Program, Princeton University, Princeton, New Jersey, USA

J. R. Toggweiler
Geophysical Fluid Dynamics Laboratory, National Oceanic and Atmospheric Administration, Princeton, New Jersey, USA

Received 23 October 2001; revised 14 June 2002; accepted 16 August 2002; published 14 February 2003.

[1] The presence of low-latitude circumglobal passage from the late Jurassic (~160 Ma) through the Miocene (~14 Ma) provides a possible mechanism for increased poleward ocean heat transport during periods of warm climate and may help explain low meridional temperature gradients of the past. Experiments using an ocean general circulation model (GCM) with an energy-balance atmosphere and idealized bathymetry reveal that, like the modern Drake Passage, a circumglobal Tethyan Passage might have induced high rates of wind-driven upwelling of relatively cold and deep water, but at low latitudes. With no change in radiative forcing, a low-latitude circumglobal passage increases simulated northern high-latitude temperatures by 3°–7°C, while tropical temperatures cool by up to 2°C relative to a scenario with solid meridional boundaries. Combining this mechanism of heat transport with increased radiative forcing allows substantial warming of northern high latitudes by 7°–11°C, while tropical temperatures remain within 3°C of present-day temperatures. *INDEX TERMS:* 3339 Meteorology and Atmospheric Dynamics: Ocean/atmosphere interactions (0312, 4504); 3344 Meteorology and Atmospheric Dynamics: Paleoclimatology; 4255 Oceanography: General: Numerical modeling; 4267 Oceanography: General: Paleoceanography; *KEYWORDS:* anoxia, Permian, extinctions, paleoceanography, stagnant, circulation

Citation: Hotinski, R. M., and J. R. Toggweiler, Impact of a Tethyan circumglobal passage on ocean heat transport and ''equable'' climates, *Paleoceanography*, *18*(1), 1007, doi:10.1029/2001PA000730, 2003.

1. Introduction

[2] Historically, paleoclimate reconstructions for the Cretaceous and early Cenozoic have indicated that high-latitude temperatures were much warmer during these periods, reaching temperatures between 10°C and 20°C, but that equatorial sea-surface temperatures were similar to or even much cooler than today's [e.g., *Shackleton and Kennett*, 1975; *Shackleton and Boersma*, 1981; *Sellwood et al.*, 1994; *Zachos et al.*, 1994; *Huber et al.*, 1995; *D'Hondt and Arthur*, 1996; *Herman and Spicer*, 1997; *Fassel and Bralower*, 1999]. Such estimates of ancient ocean temperatures rely primarily on interpretation of oxygen isotope data from foraminifera, which can be affected not only by temperature, but also by metabolic effects, the carbonate ion concentration in seawater, sea-surface $\delta^{18}O$, depth and season of calcification, and diagenesis [*Spero and Lea*, 1996; *Spero et al.*, 1997; *Norris and Wilson*, 1998; *Poulsen et al.*, 1999a; *Zeebe*, 2001]. Although these factors could contribute to underestimates of low-latitude sea-surface temperatures, *Crowley and Zachos* [2000] analyzed the combined error introduced by all effects and concluded that there is no evidence that tropical temperatures have differed significantly from Holocene reconstructed sea-surface temperatures since the Cretaceous.

Copyright 2003 by the American Geophysical Union.
0883-8305/03/2001PA000730$12.00

[3] Very recent studies of well-preserved foraminifera hosted in nearshore clay-rich sediments have concluded that tropical temperatures were similar to or warmer than present [*Norris and Wilson*, 1998; *Pearson et al.*, 2001; *Norris et al.*, 2002]. Except for the upper bound of the *Norris et al.* [2002] estimate, these nearshore data indicate tropical SST's were within 5°C of modern mean annual temperatures. Higher temperatures seem unlikely, as modern foraminiferal studies show that gametogenesis and longevity declines sharply at 32°C [*Bijma et al.*, 1990], about 5°C above modern mean annual tropical temperatures. Thus the increase in tropical temperatures was likely only ~1/3 of the increase at high latitudes.

[4] Reproducing the reduced meridional temperature gradients of the Cretaceous and Eocene has been a problem for paleoclimate modelers. Higher ancient CO_2 levels could explain past high-latitude warmth, but simulations performed with atmospheric models indicate that increased concentrations of CO_2 in the atmosphere tend to substantially warm tropical regions as well as high latitudes [*Barron and Washington*, 1982, 1985; *Manabe and Bryan*, 1985; *Schneider et al.*, 1985; *Barron et al.*, 1995; *Sloan and Rea*, 1995; *Bush and Philander*, 1997]. In atmospheric simulations with six times for modern CO_2 concentrations, high-latitude temperatures approach *minimum* values for Cretaceous and Eocene, while annual mean tropical SST's are 30°C or higher [e.g., *Sloan and Rea.*, 1995; *Barron et al.*, 1995], at the limit of even new warmer tropical temperature estimates. *Norris et al.* [2002]

suggest that warmer tropical SST's would increase tropical evaporation and latent heat transport by the atmosphere, but a coupled atmosphere/ocean simulation with 4 $\times$ CO_2 and SST's 5°C warmer than at present shows no substantial increase in poleward heat transport compared to a modern simulation [*Bush and Philander*, 1997].

[5] If reconstructed profiles are accurate indicators of past temperatures, then CO_2-induced warming was amplified at high-latitudes through either 1) cloud dynamics and vegetation albedo effects [*Kirk-Davidoff et al.*, 2002; *Sloan et al.*, 1992; *Dutton and Barron*, 1996; *Otto-Bliesner and Upchurch*, 1997; *DeConto et al.*, 2000], or 2) some mechanism that worked to transport more heat from the tropics to the poles. Since previous atmospheric simulations have failed to produce substantial increases in atmospheric poleward heat transport for Cretaceous and Early Cenozoic scenarios [*Barron and Washington*, 1982; *Manabe and Bryan*, 1985; *Bush and Philander*, 1997], attention has focused on increased ocean heat transport as the prime suspect for causing reduced meridional temperature gradients [e.g., *Covey and Barron*, 1988; *Rind and Chandler*, 1991; *Barron et al.*, 1995; *Schmidt and Mysak*, 1996; *Brady et al.*, 1998].

[6] Although simulations with reduced surface temperature gradients have yielded ocean heat transport values near those of the present-day [*Manabe and Bryan*, 1985; *Brady et al*, 1998], no satisfactory physical mechanism has been proposed for substantially *increasing* poleward ocean heat transport in the presence of the documented low gradient in sea-surface temperature (SST). Here we propose that the existence of a low-latitude circumglobal passage in the Cretaceous and Early Cenozoic may have caused a mode of ocean circulation and high poleward heat transport unique to this time period.

2. Mechanisms of Ocean Heat Transport

[7] Transport of heat poleward in the modern ocean occurs primarily through two mechanisms: thermohaline and wind-driven overturning. In the conventional thermohaline paradigm of ocean circulation, deep-water formation is balanced by widely distributed upwelling due to diffusion of heat downward. However, observations have not yielded evidence of significantly high vertical diffusivities to accomplish this overturning [*Garrett*, 1979; *Ledwell et al*, 1993; *Toole et al.*, 1994]. Because heat transport is a function of the net volume of water transported and the temperature difference between imported and exported waters for a particular latitude band, maintenance of even present heat transport through conventional thermohaline overturning would require even greater rates of vertical mixing if the meridional temperature gradient were substantially lower than today's. To reproduce early Cenozoic temperature gradients, vertical diffusion would have to have been higher by a factor of 8 [*Lyle*, 1997]. As greater rates of vertical mixing would require higher diffusivities than those that seem unrealistic for the modern day, it seems unlikely that increased diffuse upwelling would have been the cause of "equable" climates in the Mesozoic and early Cenozoic. Alternatively, *Emanuel* [2001] suggested that vertical mixing of cold water up into the mixed layer could be accomplished by tropical cyclone activity, and that a 2°C increase in tropical temperatures could increase poleward heat transport by 30% [assuming modern deep water temperatures]. With the surface-to-deep water temperature difference halved, however, it seems unlikely that increased cyclone activity could have substantially increased poleward heat transport.

[8] An alternate model of ocean overturning suggests that upwelling of deepwater occurs via wind-driven overturning in the Southern Ocean [*Toggweiler and Samuels*, 1993] rather than diffuse vertical mixing. Drake Passage, through which the Antarctic Circumpolar Current (ACC) flows, defines a narrow, longitudinally continuous zone uninterrupted by continents where no zonal pressure gradients can exist. There can therefore be no net geostrophically balanced flow across this region below the Ekman layer and above deep topography [*Gill and Bryan*, 1971; *Toggweiler and Samuels*, 1993] and equatorward Ekman flow must be primarily balanced by a deep return flow below submarine ridges. Divergence in the latitude of Drake Passage thus causes upwelling of cold deep-water, and it has been suggested that this may complete the NADW loop [*Toggweiler and Samuels*, 1993, 1995]. Because the amount of deep, cold water upwelled in the tropics is not affected, however, changes in the rate of this ocean circulation would have little effect on export of heat from low latitudes as required for the Mesozoic.

[9] Wind also drives a shallow overturning cell, with upwelling due to divergence at the equator and convergence and downwelling in subtropical gyres. This provides $\sim$40 Sv [*Watson*, 1994] of overturning; however, the heat transport this mechanism provides is limited by the latitudinal extent of the gyres, today about 30° north and south. Geographic ranges of ancient evaporites suggest that ancient wind patterns were not significantly different than modern patterns [*Gordon*, 1975; *Parrish et al.*, 1982]. Thus the influence of gyres would not have been expanded substantially poleward and changes wind-driven circulation of this type seem incapable of reducing pole-to-equator temperature gradients.

[10] Although changes in the two modern mechanisms of ocean heat transport seem insufficient to increase poleward heat flux in and of themselves, a peculiarity of the Cretaceous and early Cenozoic may have worked to combine the effects of the two modern wind-driven mechanisms to create a mode of maximal heat transport. Paleogeographic reconstructions [e.g., *Scotese et al.*, 1988, 1991] indicate that a low-latitude circumglobal passage existed during this time interval (Figure 1). Geologists have also inferred the existence of a Circumglobal Tethys Current (CTC) that flowed through this gap from migration patterns and sedimentological current indicators [*Gordon*, 1973; *Berggren and Hollister*, 1974; *Föllmi and Delamette*, 1991]. Efforts to recreate this current with general circulation models have met with mixed success, and seem to be dependent on model resolution and geography, particularly the placement of the northern margin of the Tethys ocean with respect to easterly winds [*Barron and Peterson*, 1989, 1990; *Poulsen et al.*, 1998]. However, several simulations have recreated a global westward flowing current [*Luyenduk et al.*, 1972; *Bush*, 1997; *Poulsen et al.*, 1998; *Bice and Martozke*, 2001].

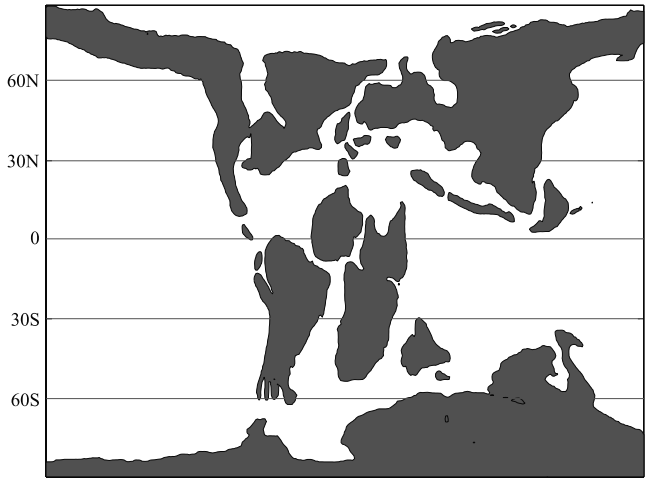

Figure 1. Early Cretaceous (110 Ma) paleogeography from Scotese (web-based data set: http://www.scotese.com). The Circumglobal Tethys Current is thought to have flowed westward through the gap that separated Asia from Africa and North America from South America.

[11] We propose that the existence of a low-latitude gap analogous to the modern-day Drake Passage would result in a merging of processes that currently occur separately at low and high-latitudes. Water upwelled at a low-latitude gap would be transported poleward like modern equatorial waters, but instead of being replaced by shallow waters from within 30° of the equator, a substantial part of the upwelled water would have to be resupplied from below ridges due to the geostrophic constraint described above for Drake Passage. This deep resupply would work to maximize heat transport in two ways. First, the temperature contrast between exported and upwelled waters would be high because waters from below ridges would be dense and likely formed in relatively cold high latitudes [*Brady et al.*, 1998; *Crowley*, 1999]. Second, the magnitude of upwelling in low latitudes would be a function of wind stress and not of density differences between high and low-latitude waters, and would therefore be sustainable in the presence of low meridional temperature gradients. Because meridional Ekman transport varies as $-\tau_x/f$ (zonal windstress divided by the Coriolis factor, which decreases toward the equator), the volume of water exported from the tropics would be much greater than the ~20 Sv of NADW postulated to upwell via the same mechanism in Drake Passage today [e.g., *Broecker*, 1991].

3. Model Description

[12] The model used is the "water planet" model of *Toggweiler and Bjornsson* [2000], which comprises a coarse resolution ocean model coupled to an energy balance model (EBM) of the Earth's atmosphere. The only differences between this simulation and those of *Toggweiler and Bjornsson* [2000] are implementation of a two-dimensional (rather than a 1-D) EBM and movement of a Drake Passage-like gap from southern high-latitudes to a position in the northern low-latitudes as described below.

[13] The atmospheric EBM is loosely based on the model of *North* [1975]. The model solves a two dimensional equation for the atmospheric heat budget where

$$C_A \cdot \frac{dT_A}{dt} = S + IR + Lateral\ Transport + Exchange\ with\ Surface,$$

where $C_A = \rho_A C_p H_A$ is the heat capacity of the atmospheric column, S is shortwave radiation absorbed by the atmosphere, and IR represents longwave radiation absorbed and emitted by the atmosphere (G. K. Vallis, personal communication, 2000) Lateral transport is assumed to follow a two-dimensional eddy diffusion law, and the atmosphere exchanges heat with the ocean surface through a sensible heat flux and radiative emission (the land surface heat capacity is assumed to be zero and the land temperatures are thus in equilibrium with radiative and sensible heat fluxes at the surface). Land and ocean albedos are fixed at a constant value in the model, thus the effects of ice are not included in this model. Latent heat fluxes are not yet implemented in the energy balance model, a point that will be addressed below in reference to model surface air temperatures and heat transport.

[14] The ocean model used is the GFDL (Geophysical Fluid Dynamics Laboratory) MOM3 general circulation model (GCM) [*Pacanowski*, 1996], with 4.5 latitudinal and 3.75 longitudinal resolution and 12 vertical levels. Mixing is parameterized using a modified version of the *Bryan and Lewis* [1979] vertical mixing scheme wherein vertical mixing varies with depth from 0.15 cm^2s^{-1} in the upper kilometer to 1.3 cm^2s^{-1} in the lowest kilometer. The model includes Gent-McWilliams parameterization of eddies (as implemented in MOM by *Griffies* [1998]).

[15] In addition to heat fluxes supplied by the EBM, surface forcing is provided by modern fixed annual mean windstresses [*Hellerman and Rosenstein*, 1983] and salt fluxes derived from the GFDL R30 coupled model [*Knutson and Manabe*, 1998]. These forcings were first zonally averaged and then averaged to be symmetric between northern and southern hemispheres (Figure 2). Previous atmospheric and coupled ocean-atmosphere GCM simulations indicate that Cretaceous winds were as strong or stronger than today [*Barron and Washington*, 1982; *Bush and Philander*, 1997], and that precipitation was (10% greater during this period of warm climate [*Bush and Philander*, 1997]. These results suggest that modern wind and salt flux estimates are reasonable forcings for the model. It should be noted that these earlier simulations exhibited elevated tropical surface air temperatures and thus sustained relatively high vertically integrated meridional temperature gradients owing to increased latent heating in low-latitudes. However, *Poulsen et al.* [1999b] found little change in wind stress upon doubling ocean heat transport in a GCM simulation of the Albian (mid-Cretaceous) atmosphere with four times modern pCO_2, despite a ~1.5°C cooling of zonally averaged sea-surface temperature [*Barron et al.*, 1993; *Poulsen et al.*, 1999b]. In addition, grain size data from aeolian dust in deep-sea cores indicate that late Cretaceous and early Cenozoic winds were comparable in intensity to modern winds [*Rea*, 1994], which suggests

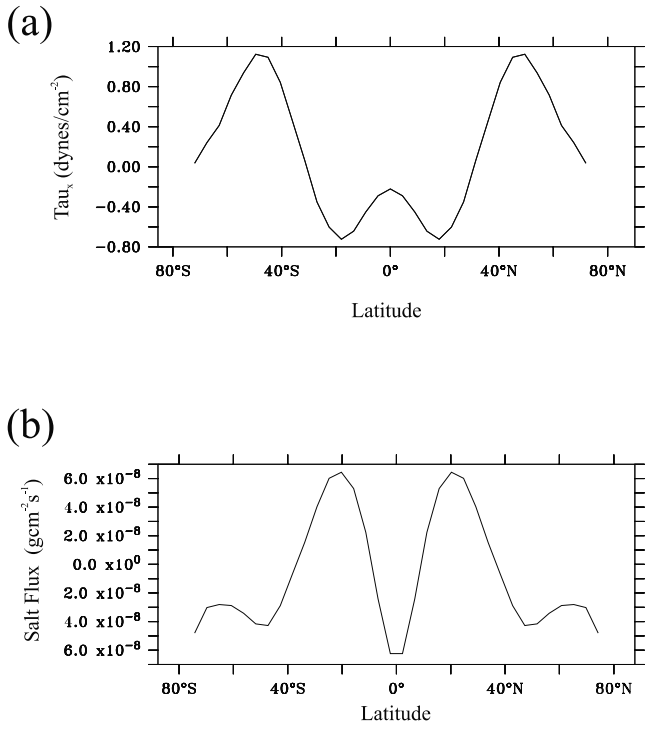

Figure 2. Surface forcings prescribed for the ocean model. Wind stress field (a) was prescribed for all experiments while salt fluxes (b) were used only in salinity-forced runs.

that present-day winds supply a reasonable forcing for simulations of warm climates.

[16] The topography of the model consists of two polar islands that extend 13.5° from each pole and thin barriers (7.5° wide) that represent continents to block flows (Figure 3). The only other features are a series of arbitrarily spaced ridges that project up from the seafloor (5000 m) to a depth of 2768 meters, which allow the formation of deep pressure gradients. Experiments were carried out with three simple model configurations, referred to as the barrier, low-latitude gap, and wandering gap scenarios. In the "barrier " experiment, which serves as our control, the water planet was configured as a single basin with a continuous barrier (Figure 3a). For the "low-latitude gap" simulation (Figure 3b), a section of the barrier from 5° to 25° north was removed, creating a longitudinally continuous 20° band of ocean unbounded by land. A second barrier was added for the "wandering gap" experiment (Figure 3c), and gaps were placed at 0°–11.25° in the first barrier and 11.25°–22.5° in the second barrier. In this "wander" scenario, there is no continuous ocean-only latitude band and a globe-encircling current would be forced to change latitudes.

[17] The highly idealized topography and bathymetry of the water planet are intended to minimize losses of momentum through lateral friction. The magnitudes of friction coefficients used in ocean GCM's are determined by the need for numerical stability, with coarser resolutions requiring higher friction coefficients. As a consequence, the large friction coefficients used in coarse-resolution models (such as the value of 2.5×10^9 cm^{2}s^{-1} in the water planet model) cause unrealistically high losses of momentum through lateral friction due to horizontal shear, particularly when strong flows interact with topography. Such frictional momentum losses allow interior flow to depart from geostrophic constraints and allow upwelling from the upper interior ocean above topography, reducing deep-sourced upwelling. By minimizing the interaction of currents with topography, the water planet model reduces departures from

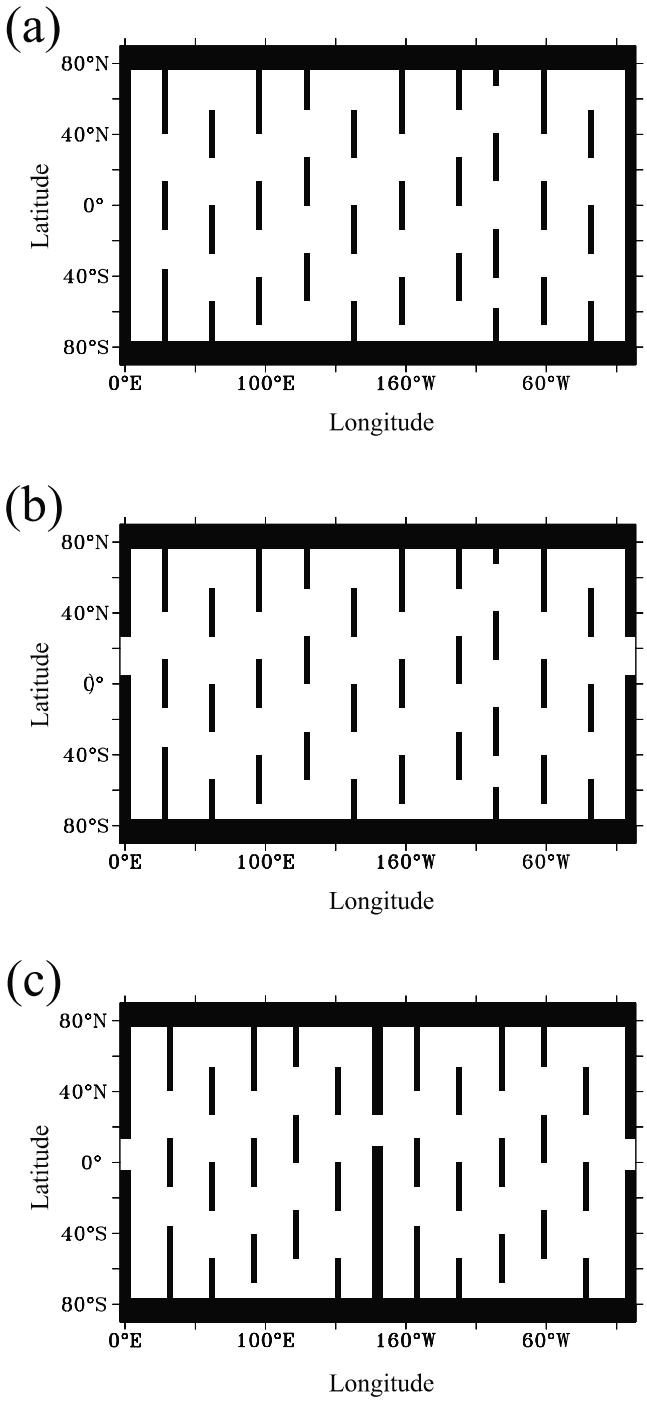

Figure 3. Basin geography and bathymetry for a) barrier, b) low-latitude gap, and c) wandering gap simulations.

geostrophy [*Toggweiler and Samuels*, 1995]. The impacts of friction will be further addressed in the Discussion (section 5.2).

4. Results

[18] The coupled model was started using the same idealized initial density profile derived from modern data for all simulations. Simulations were run for 7000 years and yielded similar global average surface air temperatures of ~14.1°C. Runs were carried out both with a constant salinity of 34.72 psu (''temperature-only'') and with salinity fluxes shown in Figure 2 (''salinity-forced).

4.1. Impact of Geography

4.1.1. Circulation and Temperature

4.1.1.1. Temperature-Only Experiment

[19] The barrier simulation with homogeneous salinities yields a circulation characterized by hemispherically symmetrical wind-driven gyres (Figure 4a), meridional overturning (Figure 4b), and temperature distributions (Figures 4c and 4d), a result consistent with *Toggweiler and Bjornsson* [2000]. Upwelling occurs near equator, but is primarily sourced from shallow, low-latitude derived waters (Figure 4b) as predicted, with <10 Sv upwelling from the deep ocean. Maximum meridional overturning in the barrier scenario is ~35 Sv and is similar in the two hemispheres. Ocean temperatures are symmetrical in cross-section, with the thermocline positioned at ~200 m depth and bowing upward at the equator (Figure 4c). Sea-surface temperatures near the pole are very cold (~−2°) and the zonal average equatorial SST is ~26°C (Figure 4d). Surface air temperatures (SAT's) follow a similar pattern, but zonal average equatorial temperatures reach only 22°C (Figure 4d). SST's are substantially higher, particularly in the tropics, due to the lack of latent heat exchange between the ocean and atmosphere in the energy balance model.

[20] Inserting a low-latitude gap in the barrier has a significant impact on ocean circulation and temperatures. Equatorial gyres are replaced by a very strong circumglobal current in the gap simulation, with a transport magnitude of 600 Sv (Figure 4e). Velocity in the center of the current is 38 cms^{-1} in the open ocean, and the current reaches a maximum velocity of 69 cms^{-1} along the southern boundary of the gap (not shown). Velocities greater than 2 cms^{-1} extend to depths of 2500 m (not shown). As in the barrier simulation, overturning circulation occurs via northern and southern cells. However, instead of being replaced primarily by shallow water as in the barrier case, low-latitude Ekman transport north of the equator is resupplied by >30 Sv of 2° water from below 2000 m with the gap in place (Figures 4f and 4g). Overall northern overturning is increased slightly to a maximum of 45 Sv, while overturning in the south is slightly stronger relative to the barrier scenario and reaches a maximum of 50 Sv.

[21] The change from shallow to deep-water resupply of equatorial waters substantially alters the ocean's temperature field from that of the barrier scenario (Figures 4g and 4h). Isotherms are substantially depressed in the northern hemisphere, which steepens the thermal gradient between northern warm water and cold water upwelling further south, and the deep ocean in both hemispheres is warmed substantially. High-latitude northern SST's and SAT's increase by ~4°C while the equator cools by ~2°C, providing a net 6° reduction in the meridional temperature gradient (Figure 4h). Because there is no change in variables that affect radiative forcing, however, tropical sea-surface cooling balances high-latitude surface warming and the globally averaged sea-surface temperature in the barrier and gap simulations is the same—~18.2°C.

4.1.1.2. Salinity-Forced Experiment

[22] Results for a run with salinity forcing are similar to those of the temperature-only simulation in a barrier scenario. In the barrier simulation with variable salinity (see Figure 2), gyre circulations are similar to those in the temperature-only barrier case (Figure 5a). Meridional overturning is reduced to 25 Sv (versus 35 in the temperature-only run) due to freshening of high-latitude surface waters relative to the temperature-only runs (not shown).

[23] Deep-water temperatures reflect this change in overturning strength and are ~4° warmer in the salinity-forced experiment due to the reduced influence of cold deepwaters (Figure 5c, see Figure 4c for comparison). In the barrier simulations polar sea-surface temperatures are cooler by 1.5 (north) and 0.8° (south) when salinity forcing is included (Figure 5d, see Figure 4d for comparison), while equatorial SST's increase by 0.25°C relative to the temperature-only run. Similarly, SAT's are cooler by −1.5°C at the northern pole and −0.6°C at the southern pole while equatorial temperatures are 0.2°C warmer in the variable-salinity barrier case.

[24] When a gap is emplaced, changes in barotropic stream function and overturning (Figures 5e and 5f) are roughly similar to those in the temperature-only experiment. The transport of the CTC is reduced to ~400 Sv in the salinity-forced scenario (Figure 5f), owing to smaller density differences across the current (not shown). Differences between northern and southern hemisphere meridional overturning, however, are enhanced in comparison with the temperature-only simulation. Whereas inclusion of a gap increased overturning in both hemispheres relative to a barrier scenario when no salinity forcing was implemented, salinity contrasts boost northern overturning to 60 Sv while reducing southern hemisphere overturning to ~20 Sv (Figure 5f). Current velocities are similar to the temperature-forced scenario.

[25] As in the barrier simulation, deepwater temperatures for the low-latitude gap scenario increase by ~4°C in the salinity-forced experiment (Figure 5g). However, the pattern of SST and SAT change induced by a circumglobal passage is similar for the temperature-only and variable-salinity experiments. Northern hemisphere warming in the salinity-forced experiment exceeds the temperature-only warming, reaching a maximum of ~7°C versus 3.5°C (Figure 5h). Equatorial temperatures cool by ~2°C relative to the salinity-forced barrier scenario while the southern hemisphere surface ocean cools by ~1°C.

[26] These results indicate that inclusion of salinity enhances the overall result of equatorial cooling accompanied by northern hemisphere warming at high latitudes.

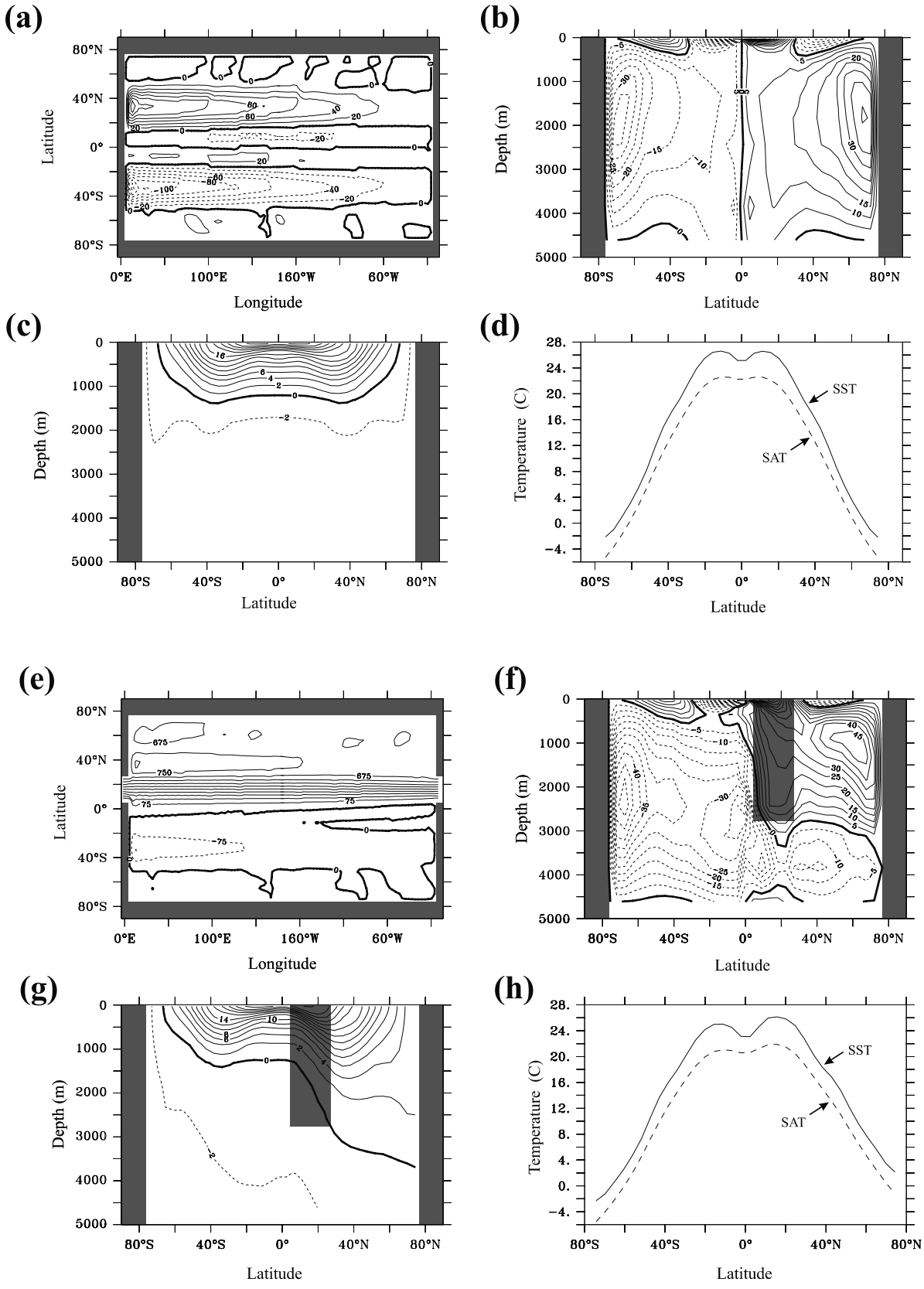

Figure 4. Results for temperature-only simulations with barrier (a, b, c, d) and low-latitude gap (e, f, g, h) configurations. Shown are barotropic stream function (a, e), meridional overturning (b, f), zonally averaged temperature profiles (c, g), and zonally averaged sea-surface and surface air temperatures (d, h).

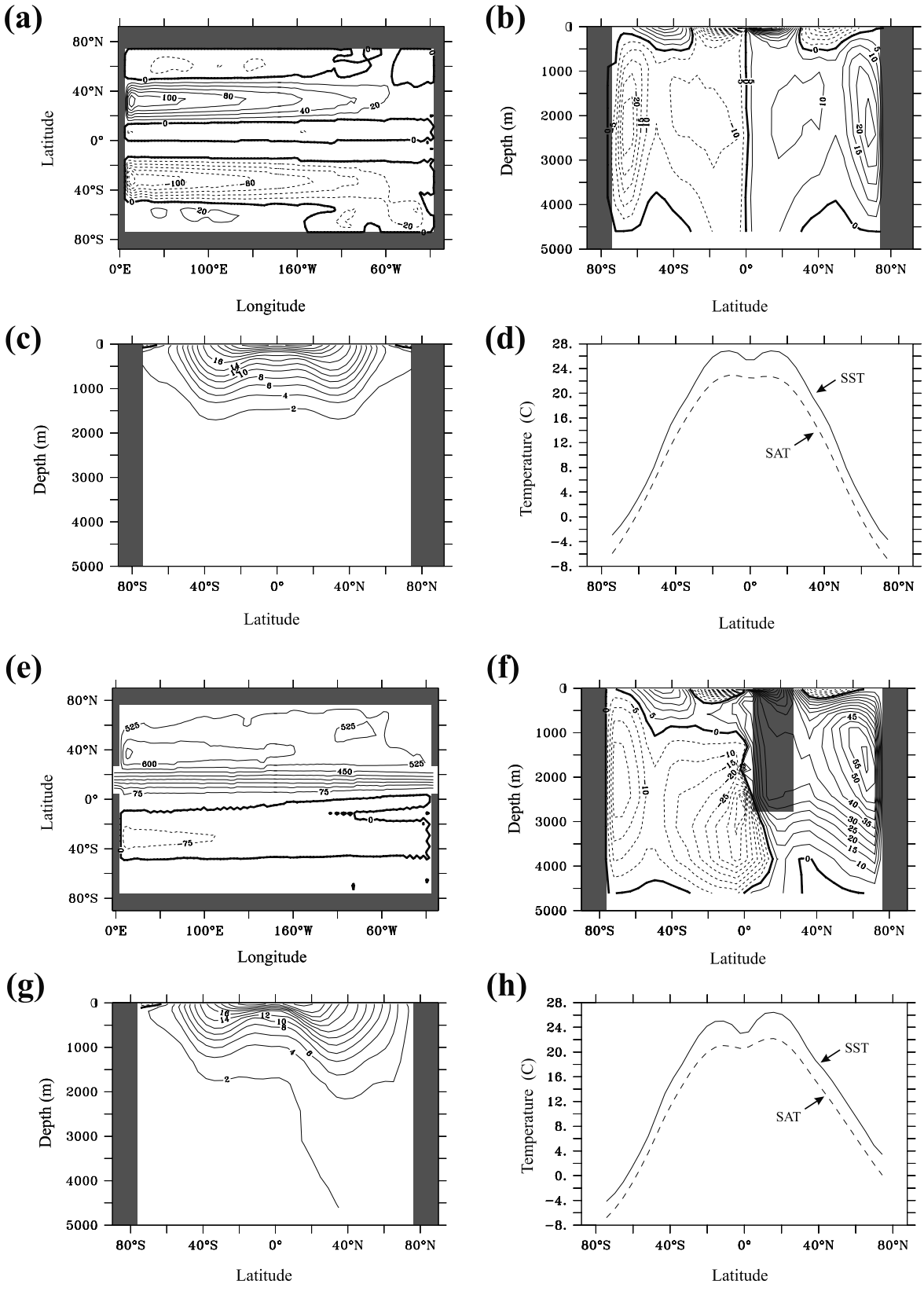

Figure 5. Results for temperature and salinity-forced simulations with barrier (a, b, c, d) and low-latitude gap (e, f, g, h) configurations. Shown are barotropic stream function (a, e), meridional overturning (b, f), zonally averaged temperature profiles (c, g), and zonally averaged sea-surface and surface air temperatures (d, h).

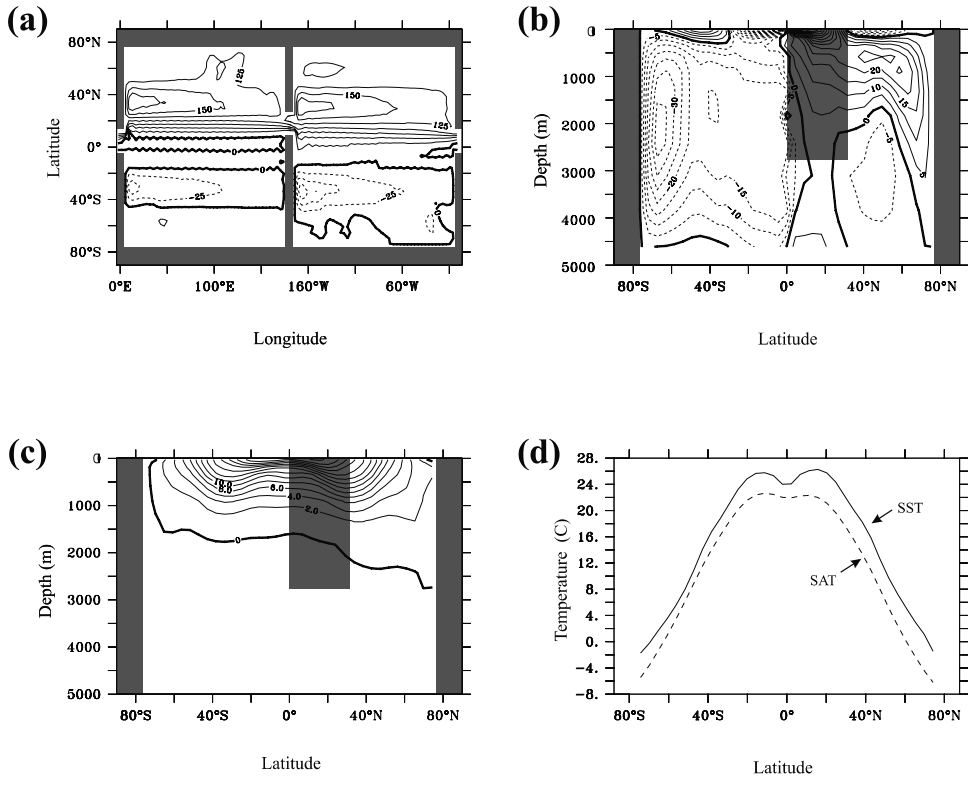

Figure 6. Results for salinity-forced simulation with a "wandering" gap configuration. Shown are barotropic stream function (a), meridional overturning (b), zonally averaged temperature profiles (c), and zonally averaged sea-surface and surface air temperatures (d).

However, the southern hemisphere cools slightly in the salinity-forced experiment due to lower meridional overturning in the south. This weak southern overturning is dictated by the presence of a strong halocline that *Toggweiler and Bjornsson* [2000] suggest inhibits deepwater formation too strongly, as the water-planet model (like all z-coordinate models) represents such formation only through convection and fails to represent cooling and sinking on high-latitude continental shelves. Thus although the result with salinity forcing may seem more "realistic," it may lead to more cooling in the southern hemisphere than warranted. Having demonstrated the sensitivity of the low-latitude gap effect to salinity, the remainder of this paper will deal with salinity-forced experiments only.

4.1.1.3. Wandering Gap Experiment

[27] Although the theoretical argument for the impact of a low-latitude gap was borne out in the low-latitude gap simulation, the circumglobal Tethyan Passage was not a straight line and the CTC would have been forced to change latitudes. To test for sensitivity to this difference, we performed a "wandering" gap experiment with two continental barriers and staggered gaps to simulate a more realistic CTC path. The two gaps are offset so that there is no circumglobally continuous latitude band on the velocity grid; the western gap extends from 0° to 11.5° north while the eastern gap extends from 11.5° to 23° north. Despite the lack of latitudinally continuous path, a circumglobal current still wends its way around the water planet in this simulation (Figure 6a). However, the frictional influence of the second barrier reduces circumglobal transport to ~120 Sv and the current extends down to only ~1500 m (not shown). Current velocities are also reduced relative to the one-gap scenario—the average open-ocean velocity is reduced to 17 cms^{-1} (from 34 cms^{-1}) and the maximum velocity reached is only 43 cms^{-1} (versus 64 cms^{-1}) (not shown).

[28] Examination of meridional overturning in the wandering gap scenario reveals that deepwater upwells through the thermocline despite the absence of a continuous ocean-only latitude band. However, upwelling is sourced by shallower water than in the one-gap simulation and the magnitude is significantly reduced from 35 Sv to 20 Sv (Figure 6b).

[29] Unlike the one-gap simulation, the deep ocean cools in the two-gap simulation relative to the barrier control case (Figure 6c, see Figure 5c for comparison). However, northern hemisphere SST changes in the two-gap scenario are still intermediate to that of the one-gap and barrier simulations, with high latitudes warming by ~3°C while temperatures at the equator are reduced by ~1.4°C relative to the barrier simulation (Figure 6d). The "wander" experiment also warms the southern hemisphere by 1.2°C. Deep low-latitude upwelling is reduced in the wandering gap experiment, which results in less heat export from low latitudes and warmer tropics, while meridional overturning in the southern hemisphere is increased and provides more heat to the southern high latitudes but cools the deep ocean. Because, as in previous experiments, there is no change in

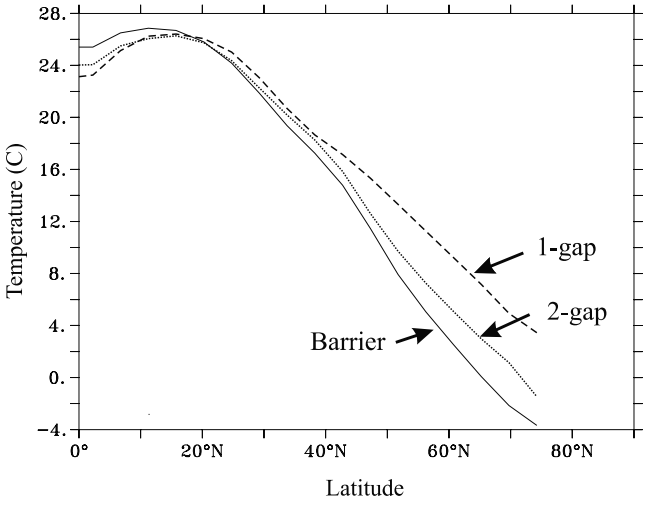

Figure 7. Summary comparison of northern hemisphere temperature zonally averaged sea-surface temperature gradients for salinity-forced simulations.

radiative forcing, the weighted mean temperature of the surface ocean cannot depart from the original equilibrium temperature; decreased northern high latitude warming does not balance tropical cooling, so southern high latitudes warm slightly. Surface air temperature changes are nearly identical to SST changes (Figure 6d).

4.1.1.4. Summary of Temperature and Circulation Changes

[30] For ease of comparison, northern hemisphere zonal sea-surface temperature gradients for salinity-forced runs are shown in Figure 7. Relative to a simulation with solid meridional boundaries, a basin configuration with a low-latitude circumglobal gap induces significantly greater upwelling of deepwater at low-latitudes and cools tropical temperatures by ~2°C while warming high latitudes by 7°C. Results are broadly similar for runs including only temperature effects and runs incorporating both temperature and salinity, although salinity forcing enhances northern hemisphere high-latitude warming. In the salinity-forced run in which the circumglobal current is forced to change latitudes, a reduction in the meridional temperature gradient still occurs but is smaller in magnitude (~1°C tropical cooling and 3°C high-latitude warming).

4.1.2. Heat Transport

[31] Poleward heat transport can be scaled as $T_o \sim V\Delta T$, where ΔT is the contrast between an average thermocline temperature and an average deepwater temperature and V is an average northward transport in the thermocline (with southward transport below) [*Fanning and Weaver*, 1997]. Total heat transport (Figure 8a) has an advective component provided by Ekman transport and geostrophic flow (Figure 8b) and a "diffusive" component supplied by isoneutral diffusion and eddy transport (Figure 8c) (note that the eddy-induced transport included in the Gent-McWilliams parameterization is included in this "diffusive" term). Maximum northern hemisphere total heat transport is 88% higher in the low-latitude gap simulation than in the barrier control case, while the "wandering" gap simulation yields a maximum total heat transport that is 35% greater that of the barrier case in the northern hemisphere (Figure 8a). The majority of the differences among the simulations are due to variations in advective heat transport for the three simulations (Figure 8b). Although Ekman heat transports are

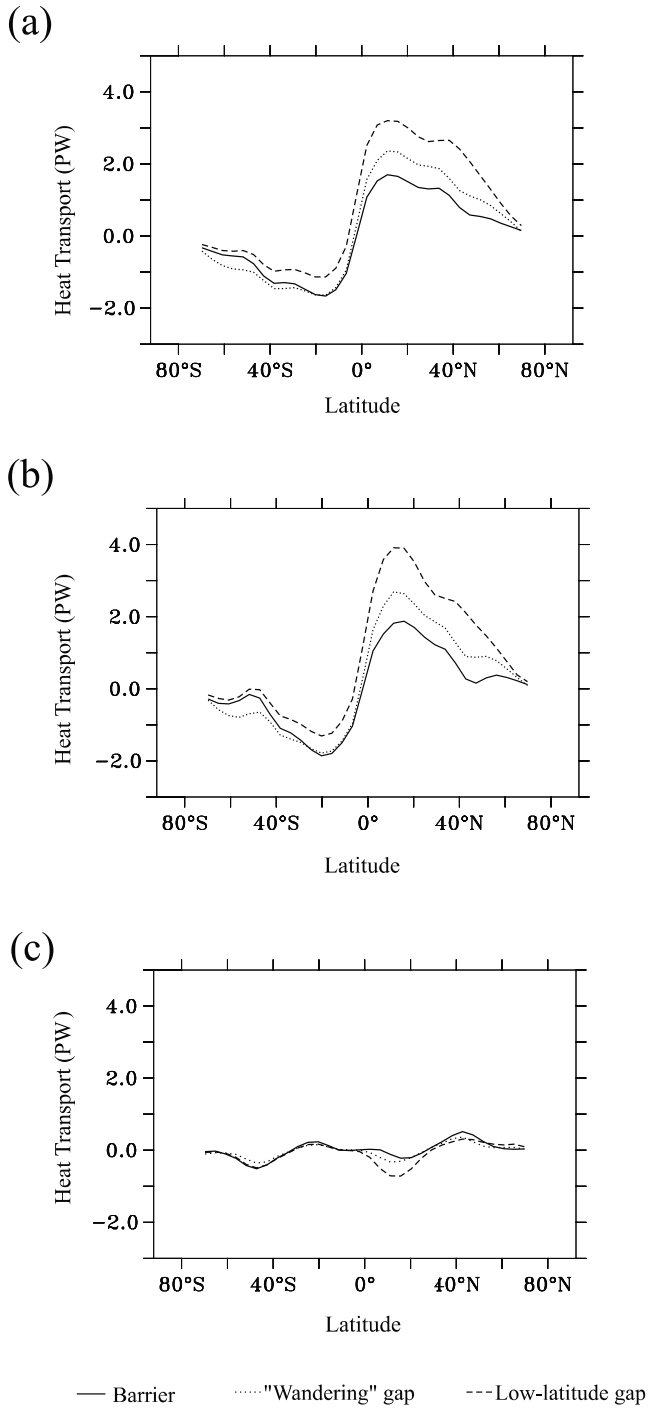

Figure 8. Total (a), advective (b), and "diffusive" (includes Gent-McWilliams eddy transport) (c) heat transport for the salinity-forced barrier (solid line), low-latitude gap (dashed line), and wandering gap (dotted line) simulations.

essentially identical for all salinity-forced simulations described above (not shown), total northern hemisphere meridional advection of heat is greater in the low-latitude gap and wandering gap scenarios due to colder temperatures of deep-sourced upwelling waters, which lead to larger ΔT and net heat transport. Transport by diffusion and eddy activity differs substantially among the three models only in low-latitudes of the northern hemisphere (Figure 8c). Isotherms become steeper equatorward in the low-latitude gap and wandering gap scenarios relative to the barrier simulation (see Figures 5c, 5g, and 5c), causing greater southward transport of heat at low latitudes. These "diffusive" transports have a relatively minor influence on total northward heat transport, but work to shift heat from the northern overturning cell to the strengthened southern cell.

[32] Because the influence of the gap does not extend appreciably to the southern hemisphere, heat transports for all simulations are very similar south of the equator and the northern hemisphere SST gradient is reduced substantially more than the southern gradient (Figures 5d, 5h, and 6d). However, these experiments are limited by the lack of interactive winds that would allow for movement of the intertropical convergence zone (ITCZ). Atmospheric GCM experiments with modern geography and a slab ocean performed by A. J. Broccoli (personal communication, 2001) may reveal a mechanism for transmitting heat from the northern to the southern hemisphere. Broccoli applied a positive heat flux anomaly to the extratropical slab ocean in the northern hemisphere and a negative heat flux heat to the southern hemisphere extratropical ocean and found that the ITCZ shifted toward the warmer hemisphere, increasing atmospheric heat transport to the cooler hemisphere extratropics via Hadley circulation. We suggest that the same mechanism could have worked on the Mesozoic and early Cenozoic Earth, helping transmit the effect of the Circumglobal Tethys passage to the southern hemisphere.

4.2. Impact of Radiative Forcing

4.2.1. Circulation and Temperature

[33] Although adding a gap warms high latitudes, high-latitude temperatures do not reach values seen for the Cretaceous and early Cenozoic. In order to test the effect of warmer bottom water on overturning and heat transport, simulations were run for 5000 years with the same forcings as in the salinity-forced cases, but with outgoing longwave radiation reduced by 4%. Using the relationship of *Myrhe et al.* [1998], this corresponds to an increase in radiative forcing supplied by an atmospheric CO_2 change to $\sim$6 times that of the control case.

[34] Results for the simulations with increased radiative forcing (henceforth "IRF") are seen in Figures 9a–9h. Surface circulation and meridional overturning for the barrier case (Figures 9a and 9b) are similar to that of the control cases (see Figures 5a and 5b). Although temperature increases are similar for all latitudes in the IRF case, maximum meridional overturning is >30 Sv, slightly greater than in the control barrier case. Deepwater temperatures are $\sim$3°C warmer than in the control barrier case (9c) and sea surface temperatures increase evenly over all latitudes (9d).

[35] Surface circulation and overturning in the two low-latitude gap cases are roughly similar (compare Figures 9e and 9f to Figures 5e and 5f) in the IRF and control cases. However, the transport of the CTC is greater than in the control case (9e–525 versus 450 Sv), due to greater density differences across the gap (not shown). In this regard the $6 \times CO_2$ experiment is more like the temperature-only experiment—in both cases increased density differences produce a faster current which results in more frictional momentum losses and shallower upwelling than in the salinity-forced gap scenario with no increase in radiative forcing. Deepwater temperatures (Figure 9g) warm by 2.1°C on average below 2000 m relative to the low-latitude control scenario and by 4.4°C relative to the control barrier experiment. SST's and SAT's (Figure 9h) increase about by a maximum of 5°C in the northern hemisphere relative to the barrier scenario with increased radiative forcing and 11°C relative to the control barrier simulation.

[36] Enhanced overturning in the barrier scenario with increased radiative forcing relative to the control is due to greater expansion of seawater at higher temperatures, which produces a larger equator-to-pole sea-surface density gradient in the IRF case (Figure 10). (This effect is similar to that noted by *Manabe and Bryan* [1985] in a simulation of enhanced pCO_2.) For the low-latitude gap simulations, however, meridional overturning in the increased forcing scenario is slightly lower (50 versus 55 Sv), despite a similar increase in sea-surface density gradient. As density gradients are similar between barrier and gap scenarios in both the control case and the IRF case, the $\sim$30 Sv greater northern meridional overturning the low-latitude gap scenarios is clearly not a function of sea-surface density. These relationships indicate that the deepwater upwelling induced in the nonradiatively forced low-latitude case is a robust feature of geography that surface wind stress and friction, rather than the surface density gradient, are the primary controls on northern hemisphere overturning in the gap simulations.

[37] Figure 11 shows a comparison of northern hemisphere results for the control and IRF simulations. When radiative forcing is increased, temperatures increase relatively evenly over all latitudes and overturning is slightly increased for the barrier scenario. In the low-latitude gap scenario, however, average tropical temperatures stay at or below 30°C while high-latitude temperatures warm by an additional 4°, for an increase of $\sim$11°C from the control barrier scenario. Southern high-latitudes, in comparison, warm by less than 4°C relative to the original barrier case (see Figures 5 and 9). Comparison of high-latitude northern temperatures in the barrier IRF case and the control case for the low-latitude gap indicate that warming induced by the gap alone is greater than that provided by an increase in

Figure 9. (opposite) Results for the salinity-forced simulations with increased radiative forcing for barrier (a, b, c, d) and low-latitude gap (e, f, g, h) configurations. Shown are barotropic stream function (a, e), meridional overturning (b, f), zonally averaged temperature profiles (c, g), and zonally averaged sea-surface and surface air temperatures (d, h).

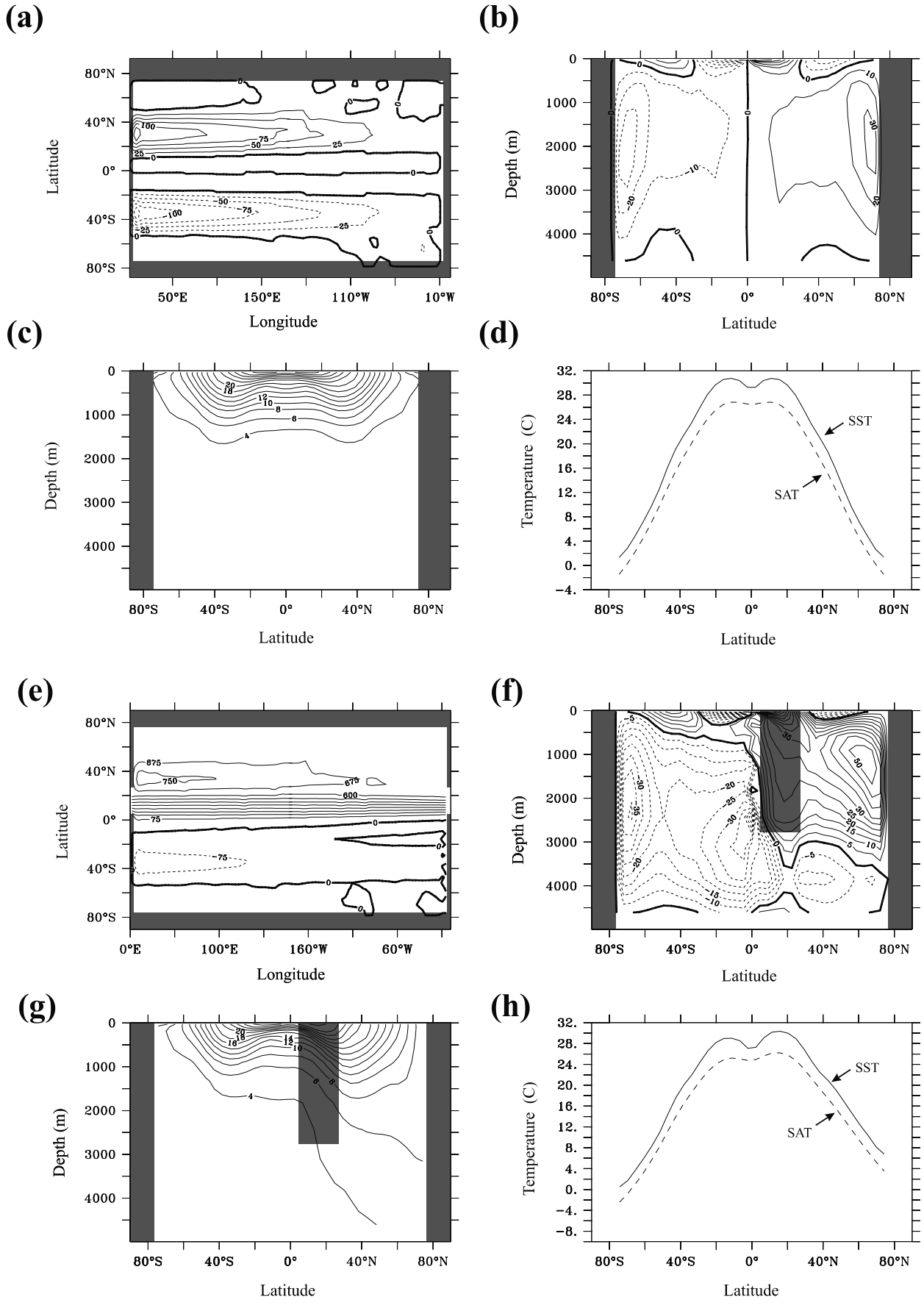
(a)
80°N
40°N
0°
40°S
80°S
Latitude
50°E
150°E
110°W
10°W
Longitude
(b)
Depth (m)
0
1000
2000
3000
4000
80°S
40°S
0°
40°N
80°N
Latitude
(c)
Depth (m)
Latitude
(d)
Temperature (C)
SST
SAT
Latitude
(e)
Latitude
0°E
100°E
160°W
60°W
Longitude
(f)
Depth (m)
Latitude
(g)
Depth (m)
Latitude
(h)
Temperature (C)
SST
SAT
Latitude

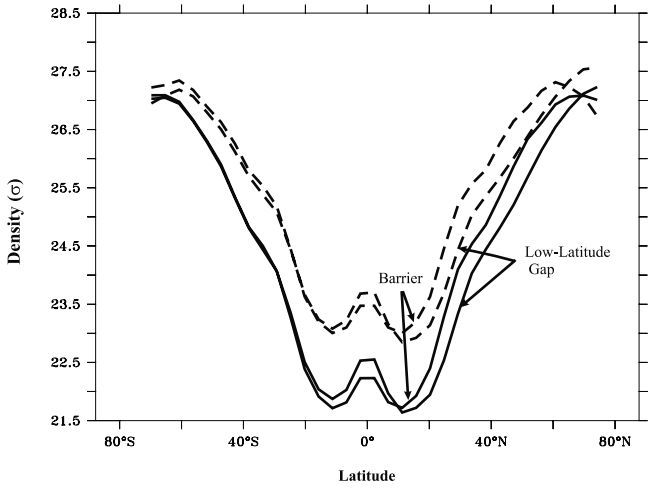

Figure 10. Plot of sea-surface density ($kg/m^3 - 1000$ kg/m^3) versus latitude in barrier and low-latitude gap simulations for control (dashed lines) and increased radiative forcing cases (solid lines).

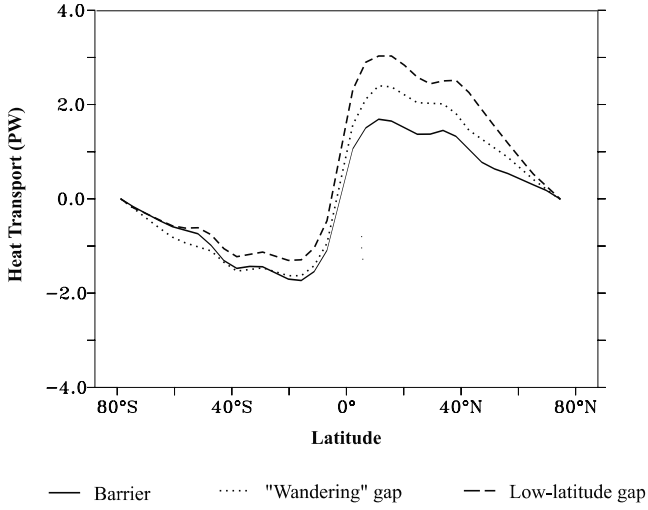

Figure 12. Comparison of northward heat transport among barrier (solid line), low-latitude gap (dashed line), and wandering gap (dotted line) simulations with increased radiative forcing (See Figure 8a for comparison with control case).

radiative forcing equal to 6 × pCO_2 alone in the barrier case (see Figure 11, shaded area). Although tropical temperatures are still cool relative to the IRF barrier scenario, zonally averaged low-latitude SST's reach up to 30.3°C at 15°N (maximum temperature is 32°C on the western side of the basin). These high temperatures are consistent with recent estimates of low-latitude and Cretaceous and early Cenozoic SST's.

[38] A simulation was also carried out for a ''wandering gap'' scenario with increased radiative forcing as in section 4.1.1.3. Results for circulation and temperature (not shown) are similar to the control case, although deepwater upwelling is reduced slightly to 20 Sv, and warming occurs in both hemispheres. Northern hemisphere temperatures increase by ~3°C relative to the barrier scenario with increased radiative forcing while the equatorial region cools by 1.2° and southern temperatures increase by 1.2°C. In comparison with the control barrier scenario, northern high latitudes warm by ~7°C.

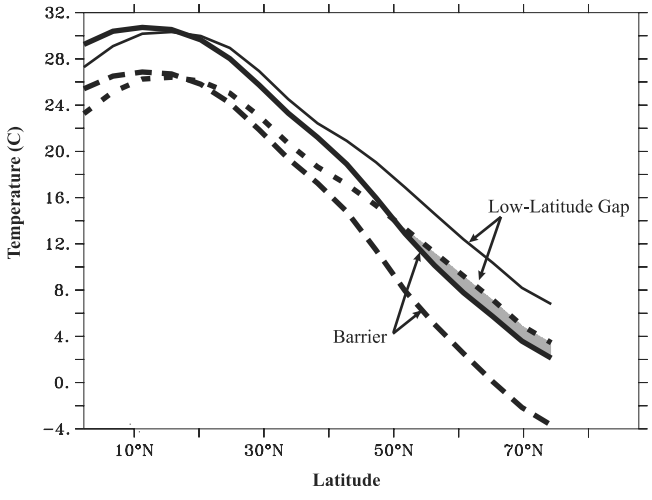

Figure 11. Northern hemisphere zonally averaged SST's for salinity-forced barrier and low-latitude gap simulations for control case (dashed lines) and increased radiative forcing case (solid lines). Shaded area indicates region where warming due to gap-induced heat transport exceeds that due to increasing radiative forcing equivalent to 6 × pCO_2 for a barrier scenario.

4.2.2. Heat Transport

[39] Figure 12 shows total poleward heat transport in the control and radiatively forced scenarios. For the barrier case, northern hemisphere poleward heat transport is slightly greater in the radiatively forced scenario (by ~0.2 PW at latitudes greater than 20°, see Figure 8a for comparison) due to a small increase in meridional overturning and maintenance of a SST gradient similar to that of the control case. Heat transport in the control and increased radiative forcing cases for the low-latitude gap scenario are also very similar. Despite increased deepwater temperatures and a substantial flattening of the meridional temperature gradient, circulation remains similar and heat transport is only ~0.2 PW lower in the northern hemisphere and ~0.2 PW higher in the southern hemisphere relative to the control case. Northern hemisphere heat transport thus remains almost twice as great as heat transport in the control barrier case. Heat transport for the IRF wandering gap case, as for the control wandering gap, is intermediate to the barrier and low-latitude IRF transports, with a maximum transport about 45% greater than the IRF barrier scenario.

5. Discussion

5.1. Timing of the Gap

[40] The Tethyan circumglobal passage was established by the Late Jurassic, reached its acme in the Late Cretaceous, and then became progressively constricted until its

closure in the Miocene [*Haq*, 1984; *Scotese et al.*, 1988; *Winterer*, 1991; *Stille et al.*, 1996; *Bill et al.*, 2001]. Neodymium isotopic signatures of phosphatic sediments indicate that Late Jurassic Tethyan and Central Atlantic ocean waters were similar to Pacific water in composition, indicating substantial flow of ocean water through the circumglobal passage at that time [*Stille et al.*, 1996]. Sedimentological indicators and foraminiferal biogeographic data suggest westward flow through the passage from the Aptian to early Cenomanian times, supporting the interpretation of circumequatorial flow [*Gordon*, 1973; *Föllmi and Delamette*, 1991]. Neodymium and carbon isotopic evidence indicate that the Circumglobal Tethyan Passage ceased to influence global ocean chemistry in the Miocene, when outflow to the Atlantic and Indian oceans ceased around between 20 Ma and 14 Ma [*Woodruff and Savin*, 1989; *Wright et al.*, 1992; *Flower and Kennett*, 1994; *Stille et al.*, 1996] due to a combination of tectonic events and/or falling sealevel [*Haq*, 1984; *Woodruff and Savin*, 1989; *Winterer*, 1991].

[41] The lifespan of the circumglobal Tethyan Passage indicated by the data above coincides with an extended period of warm climates in the Mesozoic and Paleogene. Floral evidence indicates a warming in the Late Jurassic [*Vakhrameev*, 1991] that preceded the generally warm climates of the Cretaceous, although the movement of floral boundaries may be a result of plate motion rather than global climate change [*Rees et al.*, 2000]. Temperatures increased through the Early Cretaceous, peaked in the Middle Cretaceous, then cooled through the end of the period and into the Cenozoic [e.g., *Crowley and North*, 1991]. A secondary peak of warmth occurred in the Early Eocene and was followed by a general cooling through the remainder of the late Cenozoic, punctuated by substantial cooling events in the Late Eocene, Middle Miocene, and Late Pliocene [*Miller et al.*, 1987].

[42] Evidence also suggests that the Tethys was indeed an area of high upwelling during the Cretaceous. Abundant organic carbon-rich sediments associated with positive carbon isotope excursions [e.g., *Arthur and Sageman*, 1994] and the widespread occurrence of radiolarites [e.g., *DeWever and Baudin*, 1996] indicate that productivity in the region of the CTC was high. This suggests that, at least in the Cretaceous, regional surface waters were enriched through upwelling of deep, nutrient-laden waters.

[43] The temporal coincidence of circumequatorial ocean circulation, warm climates, and strong Tethyan upwelling is consistent with the results of water-planet simulations presented above. The low-latitude gap experiments would correspond to geography in the late Jurassic and early Cretaceous, when the circumglobal passage was at its widest. By analogy to our wandering gap experiment, the increasingly tortuous path of the CTC in the Cenozoic may have resulted in reduced meridional heat transport and contributed to the cooling of ocean deep waters until its demise in the Miocene.

5.2. Contrasts With Previous Studies

[44] Given the coincidence in timing of the CTC and warm climates, together with intense interest in the role ocean heat transport in creating warm climates, it may seem unlikely that this mechanism for increased heat transport would have gone unnoticed in previous experiments. Many studies have attempted to reproduce Cretaceous and Early Cenozoic climate and ocean circulation [*Barron and Washington*, 1982; *Barron and Peterson*, 1990; *Rind and Chandler*, 1991; *Schmidt and Mysak*, 1996; *Brady et al.*, 1998; *Poulsen et al.*, 1998; *Bice and Marotzke*, 2001], but most previous models have either used fixed or restored SST's. A simulation performed by *Bush and Philander* [1997] used a coupled atmosphere-ocean model that yielded a westward-flowing Circumglobal Tethys Current but had equatorial temperatures $\sim$5°C higher than today and showed no increase in poleward ocean heat transport. This simulation, however, was only run for 32 years and did not allow sufficient time for equilibration of deep ocean temperatures and large-scale ocean overturning. A coupled model with an EBM atmosphere, in contrast to previous models, both allows runs on long timescales and allows changes in surface air temperature in response to changes in ocean heat transport.

[45] A second factor unique to our experiment is simplified geography, which reduces frictional momentum losses in the model that can allow momentum leakage at shallow depths and damp deep upwelling [*Toggweiler and Samuels*, 1995]. Although the coarse resolution of the water planet model requires a relatively large horizontal friction coefficient, the limited topography of the water planet model reduces the interaction of flows with topography, thereby reducing nongeostrophic effects in the ocean's interior. Thus although the continents of the water planet may seem unrealistic and the low-latitude gap is wider than paleoreconstructions indicate, the configuration allows for testing of mechanisms that would be masked in more "frictional" models with realistic geography and resolutions useful for long-term simulations. Because unrealistic frictional losses cannot be completely eliminated in the water planet model, however, results presented above represent lower limits to deepwater upwelling in both gap scenarios.

5.3. Reconciling Results and Records

[46] When atmospheric carbon dioxide and changes in geography are the only factors varied to reproduce high-latitude paleotemperatures, previous simulations of Cretaceous and late Paleocene climate have yielded tropical temperatures that are about 2°–5°C warmer than at present in tropical regions [*Barron et al.*, 1993, 1995; *Sloan and Rea*, 1995] while only matching minimum estimates of high-latitude temperatures. Experiments with the water planet model suggest that high-latitude warming provided by the gap-induced ocean heat transport would complement warming by elevated CO_2, reducing the magnitude of CO_2 increase (and accompanying tropical heating) needed to simulate past warm climates. In addition, the type of circulation driven by a low-latitude gap might cool the tropics by up to 2°C, significantly reducing tropical temperature increases that have accompanied increases in radiative forcing in previous experiments.

[47] When gap-induced heat transport is combined with increased radiative forcing in these experiments, zonal mean

temperature reaches 12°C at 60°N while remaining at or below 30°C in the tropics. This result is unique in that reduction of the meridional temperature gradient is achieved in an internally consistent coupled model with no specification of SST's or prescribed ocean heat transport. It should be noted that changes in meridional temperature gradient effected in the water planet model occur in the absence of latent heat transport and with simple meridional diffusion of heat. More realistic atmospheric modeling could thus further enhance tropical cooling and high-latitude warming seen here, and might provide a mechanism for warming the southern hemisphere.

6. Conclusions

[48] Simulations using a GCM with idealized geography suggest that the presence of a low-latitude circumglobal passage in the Mesozoic and early Cenozoic might have promoted wind-driven upwelling of large volumes of cold deepwater in the tropics. This mode of ocean overturning would have been independent of surface meridional temperature and density gradients and would have provided a mechanism for strong export of heat from low latitudes to polar regions. Our results are in opposition to previous interpretations of east-west gateways as barriers to northward transport of ocean waters [*Walker*, 1982; *Berggren*, 1982; *Bice et al.*, 2000].

[49] The low-latitude cooling and high-latitude warming induced by the circumglobal passage in these experiments provide a means of mitigating the classic problem of ''overheated'' tropics in GCM simulations of the Mesozoic and early Cenozoic. First, enhancement of high-latitude warming by gap-induced heat transport reduces the amount of CO_2 increase required to replicate high-latitude paleotemperatures, which would reduce accompanying tropical temperature increases. Second, increases in tropical temperatures due to higher CO_2 levels would be counteracted by upwelling-induced cooling.

[50] **Acknowledgments.** Funding for this project was provided by a NOAA Postdoctoral Fellowship in Climate and Global Change and the AOS Program of Princeton University of GFDL (Hotinski). Special thanks go to Halldor Bjornsson for model development.

References

Arthur, M. A., and B. B. Sageman, Marine black shales: Depositional mechanisms and environments of ancient deposits, *Annu. Rev. Earth Planet. Sci.*, *22*, 499–551, 1994.

Barron, E. J., and W. H. Peterson, Model simulation of the Cretaceous ocean circulation, *Science*, *244*, 684–686, 1989.

Barron, E. J., and W. H. Peterson, Mid-Cretaceous ocean circulation: Results from model sensitivity studies, *Paleoceanography*, *5*, 319–337, 1990.

Barron, E. J., and W. M. Washington, The atmospheric circulation during warm geologic periods: Is the equator-to-pole surface temperature gradient the controlling factor?, *Geology*, *10*, 633–636, 1982.

Barron, E. J., and W. M. Washington, Warm Cretaceous climates: High atmospheric CO_2 as a plausible mechanism, in *Monograph of Chapman Conference on Natural Variations in Carbon Dioxide and the Carbon Cycle*, edited by E. Sundquist and W. Broecker, pp. 546–553, AGU, Washington, D. C., 1985.

Barron, E. J., P. J. Fawcett, D. Pollard, and S. Thompson, Model simulations of Cretaceous climates: The role of geography and carbon dioxide, *Philos. Trans. R. Soc. London, Ser. B*, *341*, 307–316, 1993.

Barron, E. J., P. J. Fawcett, W. H. Peterson, D. Pollard, and S. L. Thompson, A ''simulation'' of mid-Cretaceous climate, *Paleoceanography*, *10*, 953–962, 1995.

Berggren, W. A., Role of Ocean Gateways in climatic change, in *Climate and Earth History*, pp. 118–125, Stud. Geophys., Natl. Acad. Press, Washington, D. C., 1982.

Berggren, W. A., and C. D. Hollister, Paleogeography, paleobiogeography, and the history of circulation in the Atlantic ocean, in *Studies in Oceanography*, *SEPM Spec. Publ.*, vol. 20, edited by W. W. Hay, pp. 126–186, Soc. of Econ. Paleontol. and Mineral., Tulsa, Okla., 1974.

Bice, K. L., and J. Marotzke, Numerical evidence against reversed thermohaline circulation in the warm Paleocene/Eocene ocean, *J. Geophys. Res.*, *106*, 11,529–11,542, 2001.

Bice, K. L., C. R. Scotese, D. Seidov, and E. J. Barron, Quantifying the role of geographic change in Cenozoic ocean heat transport using uncoupled atmosphere and ocean models, *Palaeogeogr. Palaeoclimatol. Palaeoecol.*, *161*, 295–310, 2000.

Bijma, J., W. W. Faber, and C. Hemleben, Temperature and salinity limits for growth and survival of some planktonic foraminifers in laboratory cultures, *J. Foraminiferal Res.*, *20*, 95–116, 1990.

Bill, M., L. O'Dogherty, J. Guex, P. O. Baumgartner, and H. Masson, Radiolarite ages in Alpine Mediterranean ophiolites: Constraints on the oceanic spreading and the Tethys-Atlantic connection, *GSA Bull.*, *113*, 129–143, 2001.

Brady, E. C., R. M. DeConto, and S. L. Thompson, Deep water formation and poleward ocean heat transport in the warm climate extreme of the Cretaceous (80 Ma), *Geophys. Res. Lett.*, *25*(22), 4205–4208, 1998.

Broecker, W. S., The Great Ocean Conveyor, *Oceanography*, *4*, 79–89, 1991.

Bryan, K., and L. Lewis, A water mass model of the world ocean, *J. Geophys. Res.*, *84*, 2503–2517, 1979.

Bush, A. B. G., Numerical simulation of the Cretaceous Tethys circumglobal current, *Science*, *275*, 807–810, 1997.

Bush, A. B. G., and S. G. H. Philander, The Late Cretaceous: Simulation with a coupled atmosphere-ocean general circulation model, *Paleoceanography*, *4*, 207–212, 1997.

Covey, C., and E. J. Barron, The role of ocean heat transport in climatic change, *Earth Sci. Rev.*, *24*, 429–445, 1988.

Crowley, T. J., Paleomyths I have known, in *Modeling the Earth's Climate and Its Variability*, edited by W. R. Holland, S. Joussame, and F. David, pp. 377–430, Elsevier Sci., New York, 1999.

Crowley, T. J., and G. R. North, *Paleoceanography*, *Oxford Monogr. Geol. Geophys.*, vol. 18, 339 pp., Oxford Univ. Press, New York, 1991.

Crowley, T. J., and J. C. Zachos, Comparison of zonal temperature profiles for past warm time periods, in *Warm Climates in Earth History*, edited by B. Huber, K. G. MacLeod, and S. L. Wing, pp. 50–76, Cambridge Univ. Press, New York, 2000.

DeConto, R. M., E. C. Brady, J. Bergengren, and W. W. Hay, Late Cretaceous climate, vegetation, and ocean interactions, in *Warm Climates in Earth History*, edited by B. Huber, K. G. MacLeod, and S. L. Wing, pp. 275–296, Cambridge Univ. Press, New York, 2000.

DeWever, P., and F. Baudin, Palaeogeography of radiolarite and organic-rich deposits in Mesozoic Tethys, *Geol. Rundsch.*, *85*, 310–326, 1996.

D'Hondt, S. D., and M. A. Arthur, Late Cretaceous oceans and the cool tropic paradox, *Science*, *271*, 1838–1841, 1996.

Dutton, J. F., and E. J. Barron, GENESIS sensitivity to changes in past vegetation, *Palaeoclimates*, *1*, 325–354, 1996.

Emanuel, K., Contributions of tropical cyclones to meridional heat transport by the oceans, *J. Geophys. Res.*, *D14*, 14,771–14,781, 2001.

Fanning, A. F., and A. J. Weaver, A horizontal resolution and parameter sensitivity study of heat transport in an idealized coupled climate model, *J. Clim.*, *10*, 2469–2478, 1997.

Fassell, M. L., and T. J. Bralower, Warm, equable mid-Cretaceous: Stable isotopic evidence, *GSA Spec. Pap.*, *332*, 121–142, 1999.

Foellmi, K. B., and M. Delamette, Model simulation of Mid-Cretaceous ocean circulation-Technical Comments, *Science*, *251*, 94, 1991.

Flower, B. P., and J. P. Kennet, The middle Miocene climatic transition: East Antractic ice sheet development, deep ocean circulation, and global carbon cycling, *Palaeogeogr. Palaeoclimatol. Palaeoecol.*, *108*, 537–555, 1994.

Garret, C., Mixing in the ocean interior, *Dyn. Atmos. Oceans*, *3*, 239–265, 1979.

Gill, A. E., and K. Bryan, Effects of geometry on the circulation of a three-dimensional southern-hemisphere ocean model, *Deep Sea Res.*, *18*, 685–721, 1971.

Gordon, W. A., Marine life and ocean surface currents in the Cretaceous, *J. Geol.*, *81*, 269–284, 1973.

Gordon, W. A., Distribution by latitude of Phanerozoic evaporite deposits, *J. Geol.*, *83*, 671–684, 1975.

Griffies, S. M., The Gent-McWilliams skew flux, *J. Phys. Oceanogr.*, *28*, 831–841, 1998.

Haq, B. U., Paleoceanography: A synoptic overview of 200 million years of ocean history, in *Marine Geology and Oceanography of Arabian Sea and Coastal Pakistan*, pp. 202–230, Van Nostrand Reinhold, New York, 1984.

Hellerman, S., and M. Rosenstein, Normal monthly windstress over the world ocean with error estimates, *J. Phys. Oceanogr.*, *28*, 831–841, 1983.

Herman, A. B., and R. A. Spicer, New quantitative palaeoclimate data for the Late Cretaceous Arctic: Evidence for a warm polar ocean, *Palaeogeogr. Palaeoclimatol. Palaeoecol.*, *128*, 227–251, 1997.

Huber, B. T., D. A. Hodell, and C. P. Hamilton, Middle-Late Cretaceous climate of the southern high latitudes: Stable isotopic evidence for minimal equator-to-pole thermal gradients, *GSA Bull.*, *107*, 1164–1191, 1995.

Kirk-Davidoff, D. B., D. P. Schrag, and J. G. Anderson, On the feedback of stratospheric clouds on polar climate, *Geophys. Res. Lett.*, *29*(11), 1556, doi:10.1029/2002GL014659, 2002.

Knutson, T. R., and S. Manabe, Model assessment of decadal variability and trends in the tropical Pacific Ocean, *J. Clim.*, *11*, 2273–2296, 1998.

Ledwell, J. R., A. J. Watson, and C. S. Law, Evidence for slow mixing across the pycnocline from an open-ocean tracer-release experiment, *Nature*, *364*, 701–703, 1993.

Luyenduk, B. P., D. Forsyth, and J. D. Phillips, Experimental approach to the paleocirculation of the oceanic surface waters, *GSA Bull.*, *83*, 2649–2664, 1972.

Lyle, M., Could Early Cenozoic thermohaline circulation have warmed the poles?, *Paleoceanography*, *12*, 161–167, 1997.

Manabe, S., and K. Bryan, CO_2-induced change in a coupled atmosphere-ocean model and its paleoclimatic implications, *J. Geophys. Res.*, *90*, 11,689–11,707, 1985.

Miller, K. G., T. R. Janecek, M. R. Katz, and D. J. Keil, Abyssal circulation and benthic foraminiferal changes near the Paleocene/Eocene boundary, *Paleoceanography*, *2*, 741–761, 1987.

Myhre, G., E. J. Highwood, K. Shine, and D. J. Stordal, New estimates of radiative forcing due to well-mixed greenhouse gases, *Geophys. Res. Lett.*, *25*(14), 2715–2718, 1998.

Norris, R. D., and P. A. Wilson, Low-latitude sea-surface temperatures for the mid-Cretaceous and the evolution of planktic foraminifera, *Geology*, *26*, 823–826, 1998.

Norris, R. D., K. L. Bice, E. A. Magno, and P. A. Wilson, Jiggling the tropical thermostat in the Cretaceous hothouse, *Geology*, *30*, 299–302, 2002.

North, G. R., Analytical solution to a simple climate model with diffusive heat transport, *J. Atmos. Sci.*, *32*, 1301–1307, 1975.

Otto-Bliesner, B. L., and G. R. Upchurch Jr., Vegetation-induced warming of high-latitude regions during the Late Cretaceous period, *Nature*, *385*, 804–807, 1997.

Pacanowski, R., MOM2: Documentation, users guide, and reference manual, Rep. 3.2, *GFDL Ocean Tech. Rep.*, Geophys. Fluid Dyn. Lab., Princeton, N. J., 1996.

Parrish, J. T., A. M. Ziegler, and C. R. Scotese, Rainfall patterns and the distribution of coals and evaporites in the Mesozoic and Cenozoic, *Palaeogeogr. Palaeoclimatol. Palaeoecol.*, *40*, 67–101, 1982.

Pearson, P. N., P. W. Ditchfield, J. Singano, K. G. Harcourt-Brown, C. J. Nicholas, R. K. Olsson, N. J. Shackleton, and M. A. Hall, Warm tropical sea surface temperatures in the Late Cretaceous and Eocene epochs, *Nature*, *413*, 481–487, 2001.

Poulsen, C. J., D. Seidov, E. J. Barron, and W. H. Peterson, The impact of paleogeographic evolution on the surface oceanic circulation and the marine environment within the mid-Cretaceous Tethys, *Paleoceanography*, *13*, 546–559, 1998.

Poulsen, C. J., E. J. Barron, and W. H. Peterson, A reinterpretation of mid-Cretaceous shallow marine temperatures through model-data comparison, *Paleoceanography*, *14*, 679–697, 1999a.

Poulsen, C. J., E. J. Barron, C. C. Johnson, and P. Fawcett, Links between major climatic factors and regional oceanic circulation in the mid-Cretaceous, in *Evolution of the Cretaceous Ocean-Climate System*, *GSA Spec. Pap.*, vol. 332, edited by E. Barrera and C. C. Johson, pp. 72–89, Geol. Soc. of Am., Boulder, Colo., 1999b.

Rea, D., The paleoclimatic record provided by eolian deposition in the deep sea: The geologic history of wind, *Rev. Geophys.*, *32*(2), 159–195, 1994.

Rees, P. M., A. M. Ziegler, and P. J. Valdes, Jurassic phytogeography and climates: New data and model comparisons, in *Warm Climates in Earth History*, edited by B. Huber, K. G. MacLeod, and S. L. Wing, pp. 297–318, Cambridge Univ. Press, New York, 2000.

Rind, D., and M. Chandler, Increased ocean heat transports and warmer climate, *J. Geophys. Res.*, *96*, 7437–7461, 1991.

Schmidt, G. A., and L. A. Mysak, Can increased poleward oceanic heat flux explain the warm Cretaceous climate?, *Paleoceanography*, *11*, 579–593, 1996.

Schneider, S. H., S. L. Thompson, and E. J. Barron, Mid-Cretaceous continental surface temperatures: Are high CO_2 concentrations needed to simulate above-freezing winter conditions? in *The Carbon Cycle and Atmospheric CO_2: Natural Variations, Archean to Present*, *Geophys. Monogr. Ser.*, vol. 32, edited by E. Sundquist and W. Broecker, pp. 554–560, AGU, Washington, D. C., 1985.

Scotese, C. R., Jurassic and Cretaceous plate tectonic reconstructions, *Palaeogeogr. Palaeoclimatol. Palaeoecol.*, *87*, 493–501, 1991.

Scotese, C. R., L. M. Gahagan, and R. L. Larson, Plate tectonic reconstructions of the Cretaceous and Cenozoic ocean basins, *Tectonophysics*, *155*, 27–48, 1988.

Sellwood, B. W., G. D. Price, and P. J. Valdes, Cooler estimates of Cretaceous temperatures, *Nature*, *370*, 453–455, 1994.

Shackleton, N. J., and A. Boersma, The climate of the Eocene ocean, *J. Geol. Soc. London*, *138*, 153–157, 1981.

Shackleton, N. J., and J. P. Kennett, Paleotemperature history of the Cenozoic and the initiation of Antarctic glaciation: Oxygen and carbon isotope analysis in DSDP sites 277, 279, and 281, in *Initial Reports of the Deep-Sea Drilling Project 29*, edited by J. P. Kennett et al., pp. 743–755, U.S. Govt. Print. Off., Washington, D. C., 1975.

Sloan, L. C., and D. K. Rea, Atmospheric carbon dioxide and early Eocene climate: A general circulation modeling sensitivity study, *Palaeogeogr. Palaeoclimatol. Palaeoecol.*, *119*, 275–292, 1995.

Sloan, L. C., J. C. G. Walker, T. C. Moore Jr., D. K. Rea, and J. C. Zachos, Possible methane-induced polar warming in the early Eocene, *Nature*, *357*, 320–322, 1992.

Spero, H. J., and D. W. Lea, Experimental determination of stable isotope variability in Globigerina bulloides: Implications for paleoceanographic reconstructions, *Mar. Micropaleontol.*, *28*(3–4), 231–246, 1996.

Spero, H. J., J. Bijma, D. W. Lea, and B. E. Bemis, Effect of seawater carbonate concentration on foraminiferal carbon and oxygen isotopes, *Nature*, *390*, 497–500, 1997.

Stille, P., M. Steinmann, and S. R. Riggs, Nd isotope evidence for the evolution of the paleocurrents in the Atlantic and Tethys Oceans during the past 180 Ma, *Earth Planet. Sci. Lett.*, *144*, 9–19, 1996.

Toggweiler, J. R., and H. Bjornsson, Drake Passage and paleoclimate, *J. Quat. Sci.*, *15*(4), 319–328, 2000.

Toggweiler, J. R., and B. L. Samuels, Is the magnitude of the deep outflow from the Atlantic Ocean actually governed by Southern Hemisphere winds? in *The Global Carbon Cycle*, *NATO ASI Ser. I*, vol. 15, edited by M. Heimann, pp. 303–331, Springer-Verlag, New York, 1993.

Toggweiler, J. R., and B. L. Samuels, Effect of Drake Passage on the global thermohaline circulation, *Deep Sea Res., Part I*, *42*, 477–500, 1995.

Toole, J. M., K. L. Polzin, and R. W. Schmitt, Estimates of diapycnal mixing in the abyssal ocean, *Science*, *264*, 1120–1123, 1994.

Vakhrameev, V. A., *Jurassic and Cretaceous Floras and Climates of the Earth*, Cambridge: Cambridge University Press, 1991.

Walker, J. C. G., Climatic factors on the Archean earth, *Palaeogeogr. Palaeoclimatol. Palaeoecol.*, *40*, 1–11, 1982.

Watson, A. J., Are upwelling zones sources of sinks of CO_2? in *Upwelling in the Ocean: Modern Processes and Ancient Records*, edited by C. P. Summerhayes et al., pp. 321–336, John Wiley, New York, 1994.

Winterer, E. L., The Tethyan Pacific during Late Jurassic and Cretaceous times, *Palaeogeog. Palaeoclimatol. Palaeoecol.*, *87*, 253–265, 1991.

Woodruff, F., and S. M. Savin, Miocene deep-water oceanography, *Paleoceanography*, *4*, 87–140, 1989.

Wright, J. D., K. G. Miller, and R. G. Fairbanks, Early and Middle Miocene stable isotopes: Implications for deepwater circulation and climate, *Paleoceanography*, *7*, 357–389, 1992.

Zachos, J. C., L. D. Stott, and K. C. Lohmann, Evolution of early Cenozoic marine temperatures, *Paleoceanography*, *9*, 353–387, 1994.

Zeebe, R. E., Seawater pH and isotopic paleotemperatures of Cretaceous oceans, *Palaeogeogr. Palaeoclimatol. Palaeoecol.*, *170*, 49–57, 2001.

R. M. Hotinski, Atmospheric and Oceanic Sciences Program, Princeton University, Princeton, NJ, USA. (hotinski@princeton.edu)

J. R. Toggweiler, Geophysical Fluid Dynamics Laboratory, National Oceanic and Atmospheric Administration, P.O. Box 308, Princeton, NJ, USA.